Desalination and Water Treatment
www.deswater.com

doi: 10.5004/dwt.2017.21052

81 (2017) 162–169
June

Performance evaluation and kinetics study of *Paracoccus versutus* and *Shinella granuli* newly isolated from pyridine-degrading aerobic granules

Wang Li, Jinyou Shen*, Xiuyun Sun, Weiqing Han, Jiansheng Li, Lianjun Wang, Xiaodong Liu*

Jiangsu Key Laboratory of Chemical Pollution Control and Resource Reuse, School of Environmental and Biological Engineering, Nanjing University of Science and Technology, Nanjing 210094, Jiangsu Province, China, Tel./Fax: +86 25 84303965; email: shenjinyou@mail.njust.edu.cn (J. Shen), Tel./Fax: +86 25 84315319; emails: liuxd@mail.njust.edu.cn (X. Liu), 1129846063@qq.com (W. Li), Tel./Fax: +86 25 84315941; email: sunxyun@mail.njust.edu.cn (X. Sun), Tel./Fax: +86 25 84315795; email: hwqxzh@sohu.com (W. Han), Tel./Fax: +86 25 84315351; email: lijsh@mail.njust.edu.cn (J. Li), Tel./Fax: +86 25 84315500; email: wanglj@mail.njust.edu.cn (L. Wang)

Received 24 January 2017; Accepted 17 June 2017

ABSTRACT

In this study, two potential pyridine-degrading strains were isolated from aerobic granules capable of degrading pyridine. The two isolates were identified and named after *Paracoccus versutus* NJUST32 and *Shinella granuli* NJUST29. Both NJUST32 and NJUST29 exhibited superior pyridine biodegradation performance, as well as high total organic carbon removal and high NH_4^+ release. Pyridine biodegradation assays showed that pyridine consumption data could be well fitted by Gompertz model, with V_{max} calculated. The q_s values calculated from V_{max} were fitted with Haldane equation, yielding q_{smax}, K_s and K_i values. For NJUST32 and NJUST29, the modeled q_{smax}, K_s and K_i were 0.3122 and 0.2180 g/g/h, 183.09 and 283.08 mg/L, and 2,457 and 1,075 mg/L, respectively. Comparing with a previously isolated pyridine degrader, namely *Rhizobium* sp. NJUST18, q_{smax} and K_i of both NJUST32 and NJUST29 were much higher than those of NJUST18, indicating higher pyridine degradation performance and lower inhibition tendency of NJUST32 and NJUST29. However, K_s values of NJUST32 and NJUST29 were significantly lower than that of *Rhizobium* sp. NJUST18, indicating higher affinity performance of these two strains toward pyridine. These results demonstrated excellent degradation performance of *P. versutus* NJUST32 and *S. granuli* NJUST29 compared with *Rhizobium* sp. NJUST18, especially at relatively high pyridine concentrations.

Keywords: Biodegradation; Kinetics; Pyridine; *Paracoccus*; *Shinella*

1. Introduction

Pyridine, a typical nitrogen heterocyclic compound, is widely used in chemical industry especially in the manufacture of dye, herbicides, pesticides and pharmaceuticals [1]. Pyridine is classified as a hazardous pollutant because of its toxic, mutagenic, carcinogenic and persistence nature [2,3]. Therefore, release of untreated pyridine-containing wastewater will cause a great damage to the ecological environment [4]. Thus, development of various efficient methods for pyridine removal is in urgent need at present.

The methods for the remediation of environment contaminated by pyridine can be divided into three categories, namely chemical, physical and biological methods. Among them, biological method is regarded to be feasible and cost-effective, showing wide application prospect [5–7]. Waston and Cain [8] first reported that pyridine could be effectively degraded by some microorganisms from soil. Subsequently, further studies showed that various bacteria were capable of degrading pyridine under both aerobic and anaerobic conditions. These strains include genera

* Corresponding author.

Arthrobacter [9], *Rhodococcus opacus* [10], *Pseudomonas* [11,12], *Shinella* [4], *Bacillus* [13], *Paracoccus* [14–16], *Streptomyces* [17], *Shewanella* [13], *Nocardiodes* [18], *Rhizobium* [19], etc. However, due to limited bacterial collections, limited information in terms of remediation strategy by pyridine-degrading strains is available now. Consequently, isolation of new strains with excellent pyridine degradation performance is still important, especially for the remediation of sites contaminated by high-strength pyridine.

Furthermore, in order to quantitatively evaluate the pyridine degradation performance of different strains, study on degradation kinetics is quite essential [20,21]. Mathur et al. [13] indicated that Monod's model could not represent the growth kinetics over the studied pyridine concentration range. However, as inhibitory growth kinetics, Haldane model could be well fitted to the growth kinetics data within the entire pyridine concentration range [22,23]. Our previous study demonstrated that both microbial growth and pyridine degradation could be well described by substrate-inhibition models, such as Haldane model [24]. However, to the best of our knowledge, kinetics on pyridine biodegradation was seldomly investigated in the previous study. Only limited information on pyridine biodegradation kinetics could be provided [13,24]. In order to understand the inhibitory tendency of pyridine toward biomass growth and pyridine degradation, it is absolutely essential to carry out the investigation of biodegradation kinetics.

Therefore, this paper aimed to isolate strains capable of degrading pyridine. Haldane model was used to describe pyridine degradation kinetics of the obtained pyridine degraders, with the related kinetics parameters revealed. In addition, pyridine degradation performance of these isolates was evaluated based on these kinetics parameters obtained in this study.

2. Materials and methods

2.1. Isolation of strains capable of degrading pyridine

Several aerobic granules were taken out from a sequencing batch reactor treating pyridine containing wastewater in our laboratory, which had been operated for more than 1 year [25]. The aerobic granules were ground and then the mixture was diluted step by step at gradient up to 10^{-10} with sterile mineral salt medium (MSM). 20 μL diluted sample were spread smoothly on Luria–Bertani (LB) agar plates supplemented with 500 mg/L pyridine. The plates were incubated at 30°C ± 2°C for 3 d. LB medium was used during incubation process in order to promote biomass growth, and pyridine was added in order to inhibit the growth of non-specific species and induce the enzymes involved in pyridine biodegradation. The colonies on LB agar plates were inoculated into liquid MSM to check their performance in terms of pyridine biodegradation. The colonies, which could grow profusely in liquid MSM with pyridine as a sole carbon and nitrogen source, were picked and restreaked for purification at least three times. Store of the isolated strains was conducted by periodical transfer and kept at –80°C with 20% glycerol in an ultralow temperature freezer.

The MSM used in this study contained KH_2PO_4 (0.38 g/L), $Na_2HPO_4{\cdot}12H_2O$ (1.53 g/L), $MgSO_4{\cdot}7H_2O$ (0.1 g/L), $CaCl_2$ (0.05 g/L) and SL-4 (10 mL/L). The composition of SL-4 was described previously [26]. Before use, MSM described above were sterilized at 121°C for 30 min in an autoclave sterilizer. Pyridine was added into the sterilized MSM at desired concentrations.

2.2. Identification of the isolated strains

Genomic DNA of isolated strains was extracted using TaKaRa MiniBEST Bacteria Genomic DNA Extraction Kit Version 3.0 according to the manufacturer's instructions. The following polymerase chain reaction (PCR) amplification was carried out with primer 1492R (5′-TACGGYTACCTTGTTACGACTT-3′) and 27F (5′-AGAGTTTG ATCCATGGCTCAG-3′). The PCR mixtures (50 μL) were composed by 0.8 μL of each primer, 25 μL of ExTaq, 21.4 μL of DEPC treated water and 2 μL template of DNA. The process was carried out under the thermocycling conditions consisted of a denaturation step at 94°C for 10 min, 30 amplification cycles of 94°C for 30 s, 55°C for 30 s, 72°C for 30 s, followed by a final extension performed at 72°C for 10 min and then kept at 25°C for 5 min on S1000™ Thermal cycler (Bio-Rad). PCR products were visualized on 1.0% agarose gels and sent for DNA sequencing. The sequence was deposited in the GenBank database, and the nucleotide sequence similarity was analyzed using BLAST program. Phylogenetic tree was constructed using neighbor-joining method based on sequences analyses with software MEGA5 [27,28].

2.3. Pyridine biodegradation assays

In order to prepare the inocula for the degradation experiment, the isolated strains were inoculated into liquid LB medium and cultivated on a shaker at 180 rpm and 30°C. In order to induce the enzymes involved in pyridine biodegradation, LB medium used during inoculum preparation was supplemented with 500 mg/L pyridine. The bacterial deposition was harvested by centrifugation at 8,000 rpm for 10 min at the end of the exponential phase (after 2 d) and then washed three times with sterile MSM. At last, bacterial suspension for the follow-up study was acquired through diluting the deposition to optical density at 600 nm (OD_{600}) of about 1.5.

For kinetics study, bacterial suspension prepared as above was inoculated into 200 mL MSM at inoculum size of 5%. The initial pyridine concentration varied from 100 to 1,500 mg/L. The cultures were incubated on a rotary shaker at 180 rpm and 30°C. During the pyridine degradation process, pyridine, NH_4^+–N and total organic carbon (TOC) concentrations were monitored at appropriate time intervals.

2.4. Kinetics model development

To quantitatively describe the pyridine degradation process, Gompertz equation was established for the calculation of biodegradation kinetics constants [29].

$$S_c = \alpha\exp(-\beta\exp(-kt)) \quad (1)$$

According to Gompertz equation, parameters such as α, β and k could be obtained by modeling the pyridine consumption data (S_c) at each initial pyridine concentration (S_i) with incubation time (t).

The corresponding maximum volumetric degradation rate (V_{max}) and time (t_{opt}) at each S_i was then calculated according to the following equation:

$$V_{max} = 0.368\ \alpha k \tag{2}$$

$$t_{opt} = \frac{\mathrm{Ln}\beta}{k} \tag{3}$$

At a given S_i, the corresponding X_{opt} at each t_{opt} could be estimated based on the yield coefficient. Finally, the specific degradation rate (q_s) at each S_i was calculated as follows:

$$q_s = \frac{V_{max}}{X_{opt}} \tag{4}$$

The Haldane equation was used to model the specific degradation rate (q_s) with initial pyridine concentration (S_i):

$$q_s = \frac{q_S^* S_i}{K_s + S_i + (S_i^2/K_i)} \tag{5}$$

Through the modeling of q_s data with S_i, fitting parameters, namely apparent maximum specific degradation rate (q_s^*), K_s and K_i, could be obtained.

According to Chrisen et al. [30], the true maximum specific degradation rate q_{smax} occurred when:

$$S_m = \sqrt{K_s K_i} \tag{6}$$

Replacing S_m in Eq. (5); Eq. (7) could be obtained:

$$q_{Smax} = \frac{q_S^*}{1 + 2\sqrt{K_s/K_i}} \tag{7}$$

In this study, the parameters of the Haldane model were obtained by a non-linear least square technique using MATLAB 7.0, based on Windows XP.

2.5. Analytical methods

Pyridine concentration was measured by a high performance liquid chromatography through authentic standard methods [31]. The mobile phase was consisted of 70% methanol and 30% ultrapure water, and pumped at a flow rate of 1.0 mL/min. NH_4^+–N concentration was measured according to Nessler's reagent colorimetric method. TOC was estimated using a Germany Elementar vario TOC analyzer. Morphology of bacteria was observed by transmission electron microscope (TEM).

3. Results and discussion

3.1. Strain isolation and identification

At least six indigenous bacterial strains able to grow with pyridine as a sole carbon and nitrogen source were isolated from pyridine aerobic degrading granules. Among them, two strains, which were named after NJUST29 and NJUST32, showed better pyridine degradation ability. Therefore, NJUST29 and NJUST32 were chosen for further study. Basic morphological characteristics of these two strains were showed in Figs. 1(a) and (b) by TEM. The morphology of NJUST32 and NJUST29 cells were rod in shape with 1.39 and 1.57 μm in length, 958 and 885 nm in width, respectively. NJUST29 was motile with one flagellum, exhibiting stronger self-aggregation ability than NJUST32 which had no flagellum. For further identification, the gene sequences of 16S rDNA of these two pyridine-degrading strains was determined and submitted to the GenBank. The sequences of NJUST29 and NJUST32 were deposited in GenBank database under accession numbers of KU051386 and KU051390, respectively. Phylogenetic tree was constructed based on the 16S rDNA sequences of the two strains and the strains showing high similarity, as indicated in Fig. 2. NJUST29 was closely related to *Shinella granuli* strain UA-STP-6, with similarity as high as 99%. NJUST32 was closely related to *Paracoccus versutus* strain ATCC 25364, with similarity as high as 99%. According to

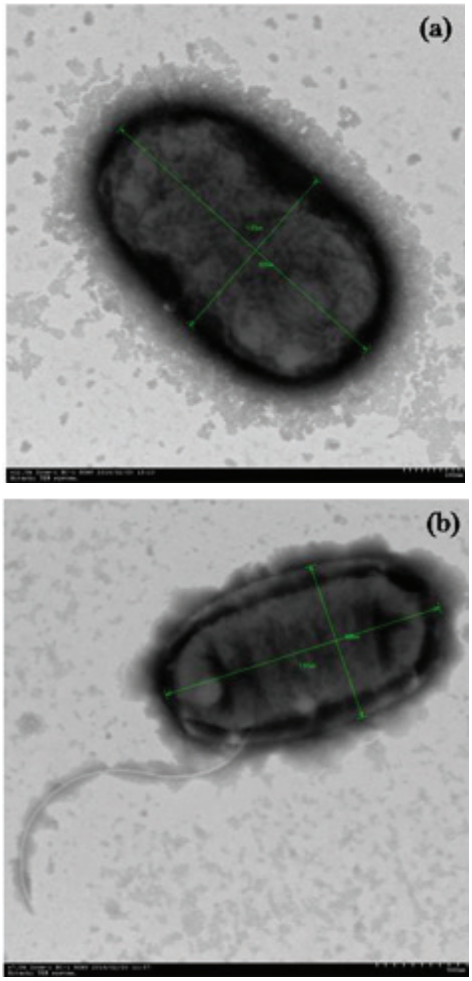

Fig. 1. Basic morphological characteristics by transmission electronic microscope of *Paracoccus versutus* NJUST32 (a) and *Shinella granuli* NJUST29 (b).

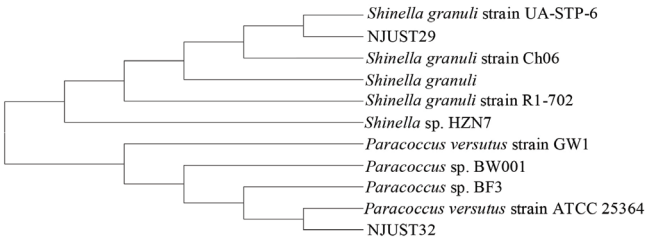

Fig. 2. Phylogenetic tree constructed by neighbour-joining method based on sequences analyses with software MEGA5.

the result of 16S rDNA sequence comparison and current taxonomic norms, NJUST29 and NJUST32 were preliminarily identified as *S. granuli* and *P. versutus*, and named after *Shinella granuli* NJUST29 and *Paracoccus versutus* NJUST32, respectively.

Currently, some bacteria belonging to *Paracoccus* and *Shinella* have been reported to be capable of degrading various recalcitrant pollutants. For example, *Paracoccus* sp. NMD-4 was found to be capable of utilizing *N*-methylpyrrolidone as the sole source of carbon and nitrogen [32]. *Paracoccus* sp. KT-5 was capable of utilizing pyridine as the sole carbon source [14]. *Shinella* sp. NJUST26 was reported to be capable of utilizing 1*H*-1,2,4-triazole as the sole carbon and nitrogen source [33]. Bai et al. [4] indicated that strain *Shinella zoogloeoides* BC026 was able to degrade pyridine efficiently. However, studies about the species *Shinella* for the removal of pyridine were seldomly reported up to now.

3.2. Pyridine biodegradation performance of NJUST29 and NJUST32

Pyridine biodegradation performance of the two new isolates, namely *S. granuli* NJUST29 and *P. versutus* NJUST32, was evaluated at initial pyridine concentration of 1,000 mg/L, as demonstrated in Fig. 3. For comparison, the performance of another pyridine-degrading strain previously isolated in our lab, namely *Rhizobium* sp. NJUST18, was also included. From Fig. 3(a), it could be seen that pyridine concentration sharply decreased after the inoculation of NJUST32, NJUST29 and NJUST18, with pyridine degradation completed within 42, 80 and 102 h, respectively. In addition, obvious biomass increases were observed in the biodegradation system inoculated with the three pyridine-degrading strains, indicating that all of the three strains were capable of utilizing pyridine as sole carbon and nitrogen source to provide their own growth.

Accompanied by pyridine biodegradation, significant NH_4^+ release was also observed in the biodegradation system inoculated with the three pyridine-degrading strains, as shown in Fig. 3(b). As reported previously, nitrogen in the pyridine ring was often transformed NH_4^+ during the process of pyridine biodegradation [14,15]. In the system inoculated with NJUST32, NJUST29 and NJUST18, final NH_4^+–N concentration was 105.65, 98.56 and 91.44 mg/L, respectively, when pyridine was completely exhausted. Correspondingly, 59.62%, 55.62% and 51.60% of the nitrogen in the pyridine ring could be converted to NH_4^+ in the biodegradation system inoculated with NJUST32, NJUST29

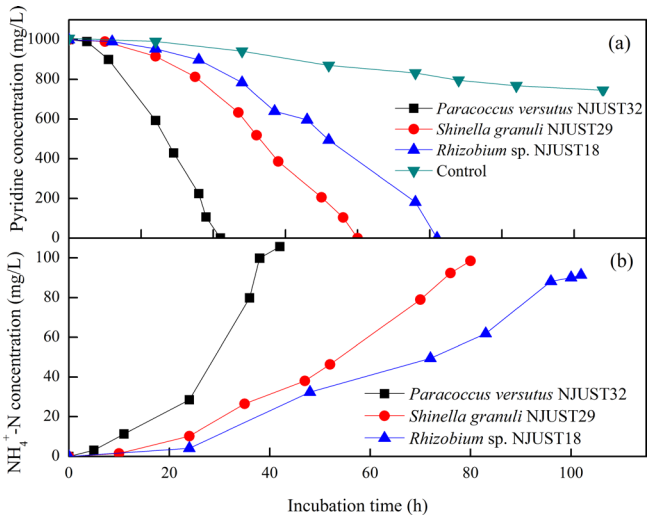

Fig. 3. Pyridine degradation (a) and NH_4^+ release (b) of *Shinella granuli* NJUST29 and *Paracoccus versutus* NJUST32.

and NJUST18, indicating the cleavage of pyridine ring. The poor mass balance for nitrogen observed in this study was probably due to the volatilization of pyridine and nitrogen loss due to biomass growth, which was also observed in the literature [14,15]. In the system inoculated with NJUST32, NJUST29 and NJUST18, TOC removal efficiencies were as high as 72.5%, 82.6% and 85.0%, respectively, when pyridine was completely exhausted, indicating the significant mineralization of pyridine in the biodegradation system inoculated by these three strains. However, among the three strains, both NH_4^+ release and residual TOC were highest in the system inoculated by NJUST32. The residual TOC concentration in biodegradation system was often dependent on the accumulation and residual of degradation intermediates. In this study, pyridine could be completely degraded within shortest incubation time by NJUST32, which would result in low volatilization of pyridine. Low volatilization of pyridine would result in more pyridine degraded, which was accompanied by relatively high residual of degradation intermediates and high NH_4^+ release. Unfortunately, the identification of biodegradation intermediates during pyridine degradation by NJUST29 and NJUST32 was unsuccessful in this study, which needs a further investigation.

In addition, clear lag phases were observed in the pyridine biodegradation systems inoculated with all of the three strains. However, short lag phase of pyridine biodegradation by NJUST32 was observed while relatively long lag phase was observed for NJUST18. Long lag phase often means high toxicity or inhibitory effect of the target contaminants toward the microorganisms involved in the biodegradation system, however, short lag phase often means high tolerance of the microorganisms toward the target contaminants [4].

Considering the significant pyridine removal, high NH_4^+ conversion, high TOC removal efficiency and high tolerance toward substrate, it could be proposed that both *S. granuli* NJUST29 and *P. versutus* NJUST32 were excellent pyridine-degrading strains, which were even superior

to *Rhizobium* sp. NJUST18. *Paracoccus* was an excellent pyridine-degrading species, which was widely reported in the literature. For example, *Paracoccus* sp. KT-5 was found to be capable of degrading 1,000 mg/L pyridine completely within 45 h [14]. *Paracoccus* sp. strain BW001 could degrade 2,614 mg/L pyridine completely within 49.5 h [15]. In a membrane bioreactor inoculated with *Paracoccus denitrificans* W12, 250–500 mg/L pyridine could be almost removed completely at hydraulic retention time of 60 h [34]. As for the species *Shinella*, it was reported that *S. zoogloeoides* BC026 was capable of degrading 1,806 mg/L pyridine completely within 45.5 h [4]. Compared with other pyridine degraders, *P. versutus* NJUST32 showed relatively high pyridine degradation ability, while *S. granuli* NJUST29 showed comparable pyridine degradation ability.

3.3. Effect of pyridine concentrations on pyridine degradation

To investigate the effect of initial pyridine concentration on pyridine biodegradation, NJUST29 and NJUST32 were cultivated in MSM within pyridine concentration ranged between 100 and 1,500 mg/L. As shown in Fig. 4(a), in the biodegradation system inoculated with NJUST32, pyridine at initial concentrations of 100, 200, 300, 400, 500, 700, 900, 1,200 and 1,500 mg/L could be degraded completely within 21, 23, 25, 26.5, 31, 33, 35, 42 and 49 h, respectively. Relatively low biodegradation efficiency was observed in the biodegradation system inoculated with NJUST29. As indicated by Fig. 4(b), at the presence of NJUST29, pyridine at initial concentrations of 100, 200, 300, 500, 600, 900 and 1,200 mg/L could be completely degraded within 43, 46, 50.5, 54, 58.5, 64 and 85 h, respectively. However, both NJUST29 and NJUST32 showed superior degradation performance than NJUST18. In the biodegradation system inoculated with NJUST18, as long as 102 h was needed for the complete removal of 1,000 mg/L pyridine. In addition, with the increase of initial pyridine concentrations, lag phases were prolonged significantly, especially in the pyridine degradation system inoculated with NJUST29. The prolonged lag phase could be attributed to the toxicity and inhibitory

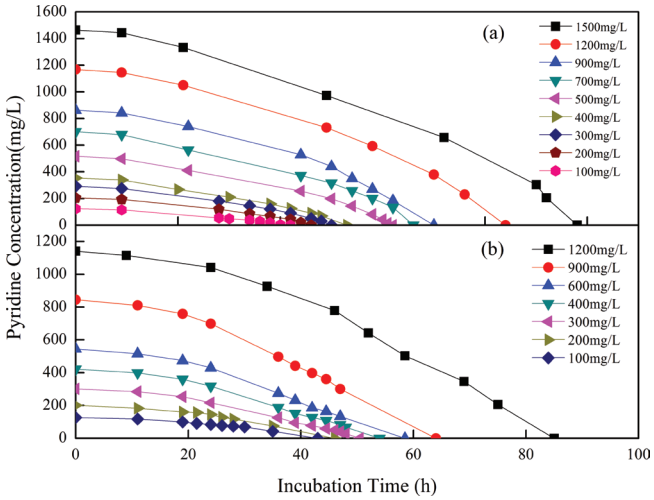

Fig. 4. Pyridine degradation profiles by *Paracoccus versutus* NJUST32 (a) and *Shinella granuli* NJUST29 (b).

effect of pyridine toward NJUST29 in biodegradation systems. The result obtained in this study indicated that both NJUST32 and NJUST29 showed higher tolerance to pyridine toxicity than NJUST18, especially for NJUST32.

3.4. Biodegradation kinetics

To further investigate the degradation performance, biomass affinity and tolerant capacity of NJUST32 and NJUST29 toward pyridine, Haldane's model was used to describe pyridine degradation kinetics to obtain true maximum specific degradation rate (q_{smax}), half saturation coefficient (K_s) and inhibition coefficient (K_i). Before that, Gompertz equation (Eq. (1)) was used to model pyridine consumption data, with fitting parameters (α, β and k) determined (R^2 ranged from 0.981 to 0.999). Then maximum volumetric degradation rate (V_{max}) and the corresponding specific degradation rate (q_s) of these two strains at each initial pyridine concentration (S_i) were calculated according to Eqs. (2)–(4), as indicated in Tables 1 and 2. For NJUST32, the calculated V_{max} increased from 8.22 to 46.28 mg/h/L with the increase of S_i from 100 to 1,500 mg/L. However, the specific degradation rate q_s displayed a substrate–inhibition behavior. The low q_s at low S_i could be attributed to the lack of carbon source, that is, pyridine. With the increase of S_i from 100 to 700 mg/L, q_s increased from 0.2205 to 0.3098 g/g/h, however, when S_i was further increased from 700 to 1,500 mg/L, q_s began to decrease from 0.3098 to 0.2919 g/g/h. Similar trend was observed in the biodegradation system inoculated with NJUST29, except that both V_{max} (ranged from 4.27 to 17.99 mg/h/L) and q_s (ranged from 0.1549 to 0.2180 g/g/h) were significantly lower than that of NJUST32.

Table 1
V_{max}, q_s for pyridine degradation by NJUST32 at different S_i

S_i (mg/L)	V_{max} (mg/h/L)	q_s (g/g/h)
100	8.22	0.2205
200	11.74	0.2482
300	14.86	0.2677
400	17.16	0.2777
500	23.01	0.3036
700	28.04	0.3098
900	31.05	0.2987
1,200	37.99	0.2983
1,500	46.28	0.2919

Table 2
V_{max}, q_s for pyridine degradation by NJUST29 at different S_i

S_i (mg/L)	V_{max} (mg/h/L)	q_s (g/g/h)
100	4.27	0.1549
200	5.61	0.1884
300	8.31	0.1929
500	10.94	0.2005
600	13.05	0.2180
900	17.99	0.2098
1,200	17.24	0.1993

As reported by other studies, for inhibitory substrates, such as phenol and pyridine, the relationship between q_s and S_i could be adequately described by Haldane's equation [24,35]. In this study, the pattern of q_s vs. S_i for NJUST32 and NJUST29 was modeled using Haldane's equation. Both experimental q_s and predicted q_s due to Haldane's equation were displayed in Figs. 5 and 6, respectively. The predicted q_s agreed well with the experimental q_s for both NJUST32 and NJUST29. It was clearly shown that a typical trend in which q_s increased initially with the increase of S_i up to a certain concentration level, then it started to decrease with the further increase of S_i. The fitting of parameters according to Haldane's equation yielded the values of apparent maximum specific degradation rate (q_s^*), q_{smax}, K_s and K_i, as shown in Table 3. The parameters of other pyridine degraders were also included in Table 3. K_i and K_s of NJUST32 and NJUST29 were found to be 2,475 and 183.1 mg/L, and 1,075 and 286.4 mg/L, respectively. q_{smax} of NJUST32 and NJUST29 was 0.3122 g/g/h at S_m of 673.2 mg/L and 0.2181 g/g/h at S_m of 551.7 mg/L, respectively, as displayed in Figs. 4 and 5. For both NJUST32 and NJUST29, the decline tendency of q_s beyond the S_m confirmed that pyridine was an inhibitory substrate and the inhibition effect pyridine toward NJUST32 and NJUST29 became predominant above 673.2 and 551.7 mg/L, respectively.

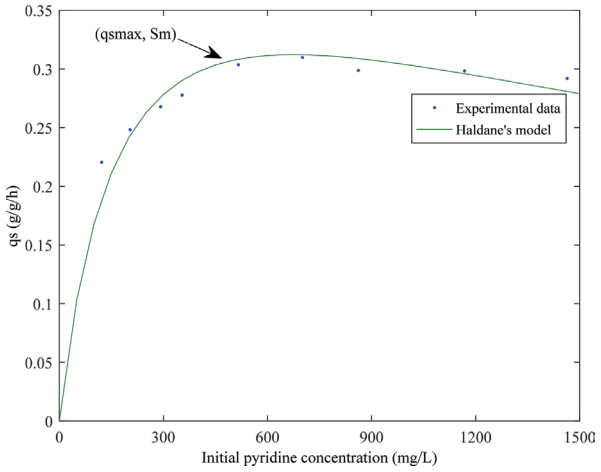

Fig. 5. Experimental and predicted specific degradation rates of *Paracoccus versutus* NJUST32 at different initial pyridine concentrations.

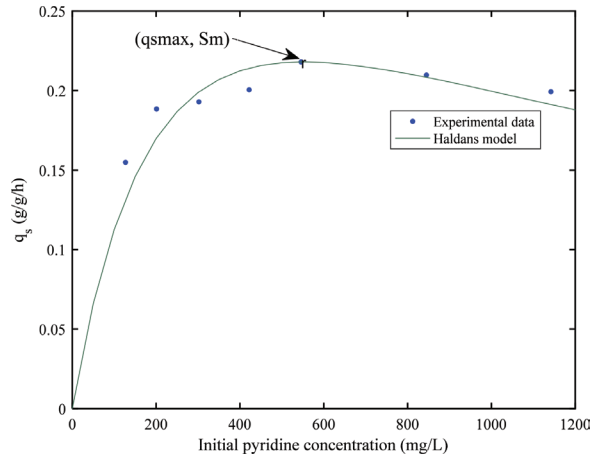

Fig. 6. Experimental and predicted specific degradation rates of *Shinella granuli* NJUST29 at different initial pyridine concentrations.

Based on biodegradation kinetics, K_i, which often indicated inhibition tendency and toxicity degree of substrates toward microorganisms, was particularly important for wastewater treatment application since it was regarded as concentration thresholds which should not be exceeded [24]. K_s, which indicated affinity of substrates toward microorganisms, directly influenced the utilization of pyridine by bacteria, especially at low residual concentrations [24]. As S_m was pyridine concentration corresponding to q_{smax}, it could be regarded as the value below which biomass growth was limited by the substrate, while above which cell growth was increasingly subject to substrate inhibition [24]. As indicated in Table 3, K_i values of both NJUST32 and NJUST29 were significantly higher than that of NJUST18, indicating that both NJUST32 and NJUST29 had stronger tolerance capacity toward pyridine. Low K_s values of NJUST32 and NJUST29 compared with NJUST18 indicated that both NJUST32 and NJUST29 had higher affinity toward pyridine. Among NJUST32, NJUST29 and NJUST18, NJUST32 showed the highest K_i and lowest K_s, indicating that NJUST32 was able to grow on pyridine within a wide pyridine concentration range, especially at relatively high pyridine concentrations. According to Table 3, both q_{smax} and S_m values of NJUST32 and NJUST29 greatly overtopped that of NJUST18, following the order of NJUST32 > NJUST29 > NJUST18. It was a direct and powerful evidence for the fact that NJUST32 had excellent pyridine degradation performance and high tolerance toward pyridine among these three strains. Both NJUST32 and NJUST29 were superior to NJUST18 in terms of pyridine biodegradation performance and tolerance toward pyridine. In a pyridine biodegradation system based on aerobic granules, q_{smax} and S_m were found to be 0.0730 g/g/h and 250.0 mg/L, respectively, which was much lower than those obtained in this study [36]. In consideration of the high q_{smax} and S_m values compared with both aerobic granules and NJUST18, the great capacities of both NJUST32 and NJUST29 in terms of high pyridine

Table 3
Pyridine biodegradation kinetics parameters by various cultures

Cultures	K_s (mg/L)	K_i (mg/L)	S_m (mg/L)	q_s^* (g/g/h)	q_{smax} (g/g/h)	Reference
NJUST32	183.1	2,475	673.2	0.4820	0.3122	This work
NJUST29	286.4	1,075	551.7	0.4420	0.2181	This work
NJUST18	558.0	462.2	507.8	0.3874	0.1212	[24]
Aerobic granules	–	–	250.00	–	0.0730	[36]

degradation rate and high tolerance toward pyridine toxicity made them adequate for the application in the treatment of pyridine containing wastewater.

4. Conclusion

In this paper, two strains capable of degrading pyridine were isolated from pyridine-degrading aerobic granules. Biodegradation performance and kinetics of these two pyridine-degrading strains was investigated and the following conclusions were derived:

- Two strains, which could utilize pyridine as the sole carbon and nitrogen source, were identified as *S. granuli* and *P. versutus*, and were named after *Shinella granuli* NJUST29 and *Paracoccus versutus* NJUST32, respectively.
- Gompertz model was successfully used to model pyridine consumption profiles. Biodegradation kinetics of NJUST29 and NJUST32 was well fitted by the Haldane's model, with kinetics parameters obtained.
- Both NJUST32 and NJUST 29 showed extremely high K_i, high q_{smax} and low K_s, indicating that these two strains had superior biodegradation performance, strong toxicity tolerance and high affinity for pyridine.

Acknowledgments

This research is financed by National Natural Science Foundation of China (No. 51478225), Natural Science Foundation of Jiangsu Province (BK20151485) and Fundamental Research Funds for the Central Universities (No. 30916011312).

Symbols

K	—	Fitting parameter of Gompertz model, h^{-1}
K_i	—	Inhibition coefficient for Haldane's degradation kinetics, mg/L
K_s	—	Half saturation coefficient for Haldane's degradation kinetics, mg/L
q_s	—	Specific degradation rate, g/g/h
q_s^*	—	Apparent maximum specific degradation rate, g/g/h
q_{smax}	—	True maximum specific degradation rate, g/g/h
S_m	—	Pyridine concentration at which $q_s = q_{smax}$, mg/L
t	—	Time of incubation, h
t_{opt}	—	Time of maximum pyridine degradation rate, h
V_{max}	—	Maximum volumetric rate of pyridine degradation, mg/L/h
X	—	Concentration of biomass, mg/L
X_{opt}	—	Concentration of biomass at t_{opt}, mg/L
α,β	—	Fitting parameter of the Gompertz model, mg/L

References

[1] S.T. Lee, S.K. Rhee, G.M. Lee, Biodegradation of pyridine by freely suspended and immobilized *Pimelobacter* sp., Appl. Microbiol. Biotechnol., 41 (1994) 652–657.
[2] J. Li, W. Cai, J. Cai, The characteristics and mechanisms of pyridine biodegradation by *Streptomyces* sp., J. Hazard. Mater., 165 (2009) 950–954.
[3] D.H. Lataye, I.M. Mishra, I.D. Mall, Removal of pyridine from aqueous solution by adsorption on bagasse fly ash, Ind. Eng. Chem. Res., 45 (2006) 3934–3943.
[4] Y. Bai, Q. Sun, C. Zhao, D. Wen, X. Tang, Aerobic degradation of pyridine by a new bacterial strain, *Shinella zoogloeoides* BC026, J. Ind. Microbiol. Biotechnol., 36 (2009) 1391–1400.
[5] J.Q. Sun, L. Xu, Y.Q. Tang, F.M. Chen, W.Q. Liu, X.L. Wu, Degradation of pyridine by one *Rhodococcus* strain in the presence of chromium (VI) or phenol, J. Hazard. Mater., 191 (2011) 62–68.
[6] H. Yun, B. Liang, J. Qiu, L. Zhang, Y. Zhao, J. Jiang, A. Wang, Functional characterization of a novel amidase involved in biotransformation of triclocarban and its dehalogenated congeners in *Ochrobactrum* sp. TCC-2, Environ. Sci. Technol., 51 (2017) 291–300.
[7] X. Jiang, J. Shen, S. Lou, Y. Mu, N. Wang, W. Han, X. Sun, J. Li, L. Wang, Comprehensive comparison of bacterial communities in a membrane-free bioelectrochemical system for removing different mononitrophenols from wastewater, Bioresour. Technol., 216 (2016) 645–652.
[8] G.K. Waston, R.B. Cain, Microbial metabolism of the pyridine ring. Metabolic pathways of pyridine biodegradation by soil bacteria, Biochem. J., 146 (1975) 157–172.
[9] E.J. O'Loughlin, G.K. Sims, S.J. Traina, Biodegradation of 2-methyl, 2-ethyl, and 2-hydroxypyridine by an *Arthrobacter* sp. isolated from subsurface sediment, Biodegradation, 10 (1999) 93–104.
[10] U. Brinkmann, W. Babel, Simultaneous utilization of pyridine and fructose by *Rhodococcus opacus* UFZ B 408 without an external nitrogen source, Appl. Microbiol. Biotechnol., 45 (1996) 217–223.
[11] S.V. Mohan, S. Sistla, R.K. Guru, K.K, Prasad, C.S. Kumar, S.V. Ramakrishna, P.N. Sarma, Microbial degradation of pyridine using *Pseudomonas* sp. and isolation of plasmid responsible for degradation, Waste Manage., 23 (2003) 167–171.
[12] R.A. Pandey, K.V. Padoley, S.S. Mukherji, S.N. Mudliar, A.N. Vaidya, A.S. Rajvaidya, T.V. Subbarao, Biotreatment of waste gas containing pyridine in a biofilter, Bioresour. Technol., 98 (2007) 2258–2267.
[13] K.A. Mathur, C.B. Majumder, S. Chatteejee, P. Roy, Biodegradation of pyridine by the new bacteril isolates *S. putrefaciens* and *B. sphaericus*, J. Hazard. Mater., 157 (2008) 335–343.
[14] L. Qiao, J.L. Wang, Microbial degradation of pyridine by *Paracoccus* sp. isolated from contaminated soil, J. Hazard. Mater., 176 (2010) 220–225.
[15] Y. Bai, Q. Sun, C. Zhao, D. Wen, X. Tang, Microbial degradation and metabolic pathway of pyridine by a *Paracoccus* sp. strain BW001, Biodegradation, 19 (2008) 915–926.
[16] L. Qiao, D. Wen, J. Wang, Biodegradation of pyridine by *Paracoccus* sp. KT-5 immobilized on bamboo-based activated carbon, Bioresour. Technol., 101 (2010) 5229–5234.
[17] J. Li, W. Cai, J. Cai, The characteristics and mechanisms of pyridine biodegradation by *Streptomyces* sp., J. Hazard. Mater., 165 (2009) 950–954.
[18] S.K. Rhee, K.Y. Lee, J.C. Chung, S.T. Lee, Degradation of pyridine by *Nocardioides* sp. strain OS4 isolated from the oxic zone of a spent shale column, Can. J. Microbiol., 43 (1997) 205–209.
[19] J. Shen, X. Zhang, D. Chen, X. Liu, L. Wang, Characteristics of pyridine biodegradation by a novel bacterial strain, *Rhizobium* sp. NJUST18, Desal. Wat. Treat., 53 (2015) 2005–2013.
[20] J. Bai, J.P. Wen, H.M. Li, Y. Jiang, Kinetic modeling of growth and biodegradation of phenol and *m*-cresol using *Alcaligenes faecalis*, Process Biochem., 42 (2007) 510–517.
[21] K.C. Loh, Y.G. Yu, Kinetics of carbazole degradation by *Pseudomonas putida* in presence of sodium salicylate, Water Res., 34 (2000) 4131–4138.
[22] A. Kumar, S. Kumar, S. Kumar, Biodegradation kinetics of phenol and catechol using *Pseudomonas putida* MTCC 1194, Biochem. Eng. J., 22 (2005) 151–159.
[23] S. Tsai, C. Lin, C. Wu, C. Shen, Kinetics of xenobiotic biodegradation by the *Pseudomonas* sp. YATO411 strain in suspension and cell-immobilized beads, J. Taiwan Inst. Chem. Eng., 44 (2013) 303–309.

[24] J. Shen, X. Zhang, D. Chen, X. Liu, X. Sun, J. Li, H. Bi, L. Wang, Kinetics study of pyridine biodegradation by a novel bacterial strain, *Rhizobium* sp. NJUST18, Bioprocess Biosyst. Eng., 37 (2014) 1185–1192.
[25] X. Liu, Y. Chen, X. Zhang, X. Jiang, S. Wu, J. Shen, X. Sun, J. Li, L. Lu, L. Wang, Aerobic granulation strategy for bioaugmentation of a sequencing batch reactor (SBR) treating high strength pyridine wastewater, J. Hazard. Mater., 295 (2015) 153–160.
[26] J. Shen, J. Zhang, Y. Zuo, L. Wang, X. Sun, J. Li, W. Han, Biodegradation of 2,4,6-trinitrophenol by *Rhodococcus* sp. isolated from a picric acid-contaminated soil, J. Hazard. Mater., 163 (2009) 1199–1206.
[27] N. Saitou, M. Nei, The neighbor-joining method: a new method for reconstructing phylogenetic trees, Mol. Biol. Evol., 4 (1987) 406–425.
[28] S. Kumar, K. Tamura, M. Nei, MEGA3: integrated software for molecular evolutionary genetics analysis and sequence alignment, Briefings Bioinf., 5 (2004) 150–163.
[29] M.E. Acuna, F. Perez, R. Auria, S. Revah, Microbiological and kinetic aspects of a biofilter for the removal of toluene from waste gases, Biotechnol. Bioeng., 63 (1999) 175–184.
[30] P. Chrisen, A. Vega, L. Casalot, G. Simon, R. Auria, Kinetics of aerobic phenol biodegradation by the acidophilic and hyperthermophilic archaeon *Sulfolobus solfataricus* 98/2, Biochem. Eng. J., 62 (2012) 56–61.
[31] J. Shen, Y. Chen, S. Wu, H. Wu, X. Liu, X. Sun, J. Li, L. Wang, Enhanced pyridine biodegradation under anoxic condition: the key role of nitrate as the electron acceptor, Chem. Eng. J., 277 (2015) 140–149.
[32] S. Cai, T. Cai, S. Liu, Q. Yang, J. He, L. Chen, J. Hu, Biodegradation of N-methylpyrrolidone by *Paracoccus* sp. NMD-4 and its degradation pathway, Int. Biodeterior. Biodegrad., 93 (2014) 70–77.
[33] H. Wu, J. Shen, R. Wu, X. Sun, J. Li, W. Han, L. Wang, Biodegradation mechanism of 1H-1,2,4-triazole by a newly isolated strain *Shinella* sp. NJUST26, Sci. Rep., 6 (2016) 29675.
[34] D. Wen, J. Zhang, R. Xiong, R. Liu, L. Chen, Bioaugmentation with a pyridine-degrading bacterium in a membrane bioreactor treating pharmaceutical wastewater, J. Environ. Sci., 25 (2013) 2265–2271.
[35] J. Shen, R. He, J. Zhang, Y. Zuo, Y. Li, X. Sun, J. Li, L. Wang, W. Han, Biodegradation kinetics of picric acid by *Rhodococcus* sp. NJUST16 in batch reactors, J. Hazard. Mater., 167 (2009) 193–198.
[36] S.S. Adav, D.J. Lee, N.Q. Ren, Biodegradation of pyridine using aerobic granules in the presence of phenol, Water Res., 41 (2007) 2903–2910.